

# Effect of Temperature on the Reaction of HO• with Benzene and Pentahalogenated Phenolate Anions in Subcritical and Supercritical Water

John L. Ferry and Marye Anne Fox\*

Department of Chemistry and Biochemistry, University of Texas at Austin, Austin, Texas 78712

Received: October 28, 1997; In Final Form: March 17, 1998

The effect of temperature, from ambient to supercritical, on the products of the reaction in water of HO• with benzene and the anions of pentabromophenol, pentachlorophenol, and pentafluorophenol is reported. Increasing temperature favored one-electron oxidation of the perbrominated and perchlorinated phenolate anions over adduct formation, yielding the corresponding phenoxyl radicals. In contrast, with benzene and pentafluorophenolate, the corresponding hydroxyl radical adduct was formed. The bimolecular rate constant for the self-reaction of the hydroxycyclohexadienyl radical was measured and its temperature dependence determined: for benzene, a kinetic analysis gave  $E_a$  of 48.0 kJ/mol and a preexponential term of  $7.42 \times 10^{14} \text{ M}^{-1} \text{ s}^{-1}$ . The temperature dependence for the rate constant of the decay of the pentabromophenoxyl radical was non-Arrhenius, with a significant change in mechanism taking place at approximately 200 °C.

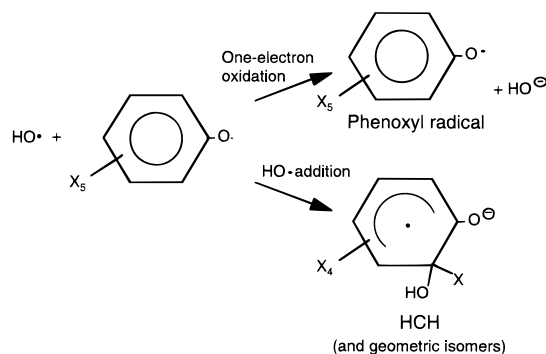
## Introduction

The dioxygen-mediated oxidation of organic compounds in subcritical and supercritical water ( $T_c$  374.2 °C,  $P_c$  = 3160 psia) is thought to involve the intermediacy of hydroxyl (HO•) and hydroperoxyl (HOO•) radicals.<sup>1,2</sup> This assumption is based on the products resulting from the partial oxidation of several different families of organic compounds. For example, Gopalan and Savage found that the oxidation of phenol in supercritical water took place by coupling to produce dihydroxybiphenyls, followed by ring opening to produce carboxylic acids,<sup>3</sup> and Crain and co-workers observed the formation of hydroxypyridine and low-molecular-weight organic acids from the oxidation of pyridine.<sup>4</sup>

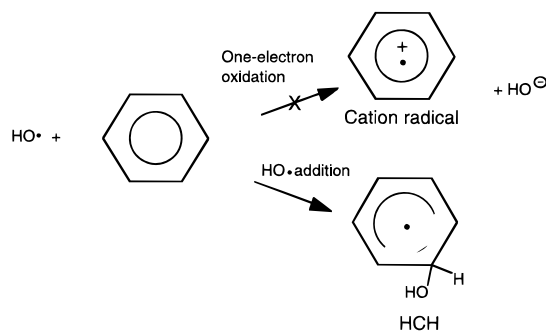
The kinetics and products of the reactions between the anions of substituted phenols and hydroxyl radical (HO•) have been well studied at 25 °C.<sup>5,6</sup> Two different pathways are possible: (1) one-electron oxidation to produce a phenoxyl radical or (2) addition of hydroxyl radical to the ring, forming a hydroxycyclohexadienyl radical (HCH), Scheme 1. In contrast, at room temperature, simple aromatic molecules such as benzene form the HCH radical in 100% yield, Scheme 2.<sup>7</sup> No evidence for one-electron oxidation to produce a cation radical has been observed in water except at very low pH (<1).<sup>8</sup> The phenoxyl and HCH radicals produced by these routes decay through bimolecular processes (in the absence of oxygen) at room temperature, coupling to produce primarily dihydroxybiphenyls<sup>9,10</sup> or participating in disproportionation.<sup>11</sup> At elevated temperatures, phenoxyl radicals may also decompose unimolecularly to lose CO and form the corresponding cyclopentadienyl radical.<sup>12</sup>

The high solubility of organic compounds and dioxygen in near-critical and supercritical water makes these environments a suitable medium for either the oxidation of hazardous waste or the controlled synthesis of organic chemicals.<sup>13–15</sup> Certain properties of the high-temperature fluid, e.g., its dielectric constant, can be adjusted by varying the external pressure, especially near the critical point. This can have a significant impact on the partitioning among competing reactions.<sup>16</sup> For example, by adjusting the dielectric constant of the medium,

**SCHEME 1: Reactions between HO• and Substituted Phenolate Anions (X = H, Br, Cl, or F) in Aqueous Solution**



**SCHEME 2: Reactions between HO• and Benzene in Aqueous Solution**



Hrnjez and co-workers were able to influence the product distribution of the photochemical dimerization of isophorone in supercritical HCF<sub>3</sub> and in supercritical CO<sub>2</sub>, with the polar head-to-head dimer being favored at high dielectric constant.<sup>16</sup> Changes in the dielectric constant of water (from 80 to 1.7 upon proceeding from standard conditions to 400 °C at 3600 psia) should induce pronounced effects on the product distribution obtained from reactions with marked differences in transition-state polarity.<sup>17</sup>

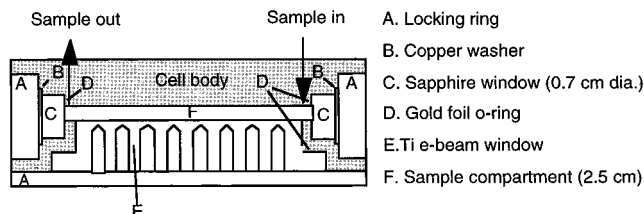


**Figure 1.** Cut-away top view of the high-pressure, high-temperature e-beam cell.

In this study, the decay kinetics of the transient phenoxy and HCH radicals derived from the HO<sup>•</sup>-mediated oxidation of aqueous pentabromophenolate, pentachlorophenolate, and pentafluorophenolate anions and of benzene are used to probe the effects of temperature on the initial oxidations of these compounds in subcritical and supercritical water.

### Experimental Section

**Materials.** Benzene (99.5%), pentafluorophenol (98%), pentachlorophenol (99%), pentabromophenol (99+%), L-ascorbic acid (99+%), dibasic phosphate (99%), NaOH (99%), NaN<sub>3</sub> (99.5%), and KSCN (99%) (Aldrich) were used as received. Water was ASTM grade ( $\geq 15.7$  M $\Omega$ ) supplied by a Milli-Q filtration system.

**Electron Accelerator.** The pulse radiolysis experiments were performed with a 4 MeV van de Graff accelerator, with a pulse width of 1  $\mu$ s. Transient absorptions were measured using a 250 W xenon lamp, grating monochromator, and photomultiplier arrangement, as described earlier.<sup>5</sup> Aqueous KSCN (0.080 M) was used for dosimetry. Using the known absorbance of (SCN)<sub>2</sub><sup>•-</sup> at 480 ( $\epsilon_{480}$  7600 M<sup>-1</sup> cm<sup>-1</sup>),<sup>5</sup> the yield of HO<sup>•</sup> was determined to vary between  $5.23 \times 10^{-6}$  and  $5.76 \times 10^{-6}$  M per pulse. Pulse energy was maintained at this level and monitored continuously with a relative energy monitor. The time dependence of the absorption spectra was recorded on a Biomation 8100 digitizer interface interfaced with an Acer 386SX PC for data analysis.

**Radiolysis Cell.** Pulse radiolysis was carried out in a Ti (type II) flow-through cell fitted with sapphire windows for optical monitoring. The electron beam passed through a Ti "window", a solid plug of Ti inserted into the cell with drilled thin spots analogous to previously described steel electron beam win-

dows.<sup>18,19</sup> A cross-sectional view of the cell is given in Figure 1, and a schematic of the pressurization assembly is provided in Figure 2. The total volume of the cell was 300  $\mu$ L.

Pressure was maintained to within  $\pm 50$  psia as monitored by a Heisse digital pressure gauge. Temperature was monitored by a J-type thermocouple inserted into the body of the cell and read by an Omega temperature controller. The system was pressurized by a Waters 510 HPLC pump followed by a Swagelok R134 pressure relief valve for pressure control. Flow rates varying between 0.1 mL/min (at temperatures below 200 °C) and 1.0 mL/min (above 200 °C) gave hydraulic retention times of 20 s at high temperature. This was done to minimize possible thermohydrolysis of the substrates, which, in the absence of dioxygen, has been shown to be slow for most organic molecules, occurring on a time scale of several minutes even for such labile compounds as aromatic ethers.<sup>20,21</sup> In addition, no transient absorptions attributable to Br<sub>2</sub><sup>•-</sup> or Cl<sub>2</sub><sup>•-</sup> were detected, demonstrating that pentachlorophenol and pentabromophenol were inert toward thermal hydrolysis over this time scale.

**Solution Preparation.** A saturated aqueous solution of benzene was stored under N<sub>2</sub>O. This stock solution was diluted to the appropriate concentration with Milli-Q water that had been deaerated and saturated with N<sub>2</sub>O. During the experiments, a gentle stream of N<sub>2</sub>O was passed slowly over this solution (to prevent oxygen contamination and to avoid stripping the benzene).

The substituted phenolate anion solutions were prepared by dissolving the neat phenol in 500  $\mu$ M dibasic phosphate, and additional pH adjustment was accomplished by adding concentrated NaOH, to a minimum of pH 8.5. The pK<sub>a</sub> of pentachlorophenol is 4.5, and the pK<sub>a</sub> of pentafluorophenol is 5.5 (pentabromophenol is insoluble in water),<sup>5</sup> so the substrates were present as phenolate anions rather than the protonated forms even at high temperatures.<sup>22</sup> These solutions were degassed by bubbling with N<sub>2</sub>O for a minimum of 45 min before and throughout the experiments.

### Results and Discussion

Pulse radiolysis was used to generate HO<sup>•</sup>.<sup>23</sup> Electron bombardment of aqueous solutions results in the production of several different transient and stable products through a manifold

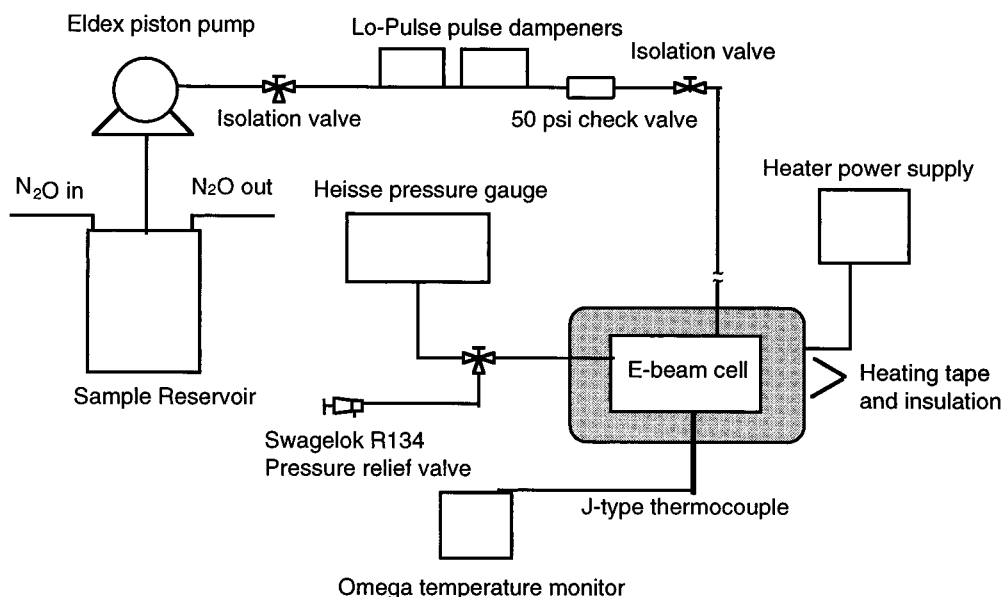


**Figure 2.** Block diagram of the cell assembly.

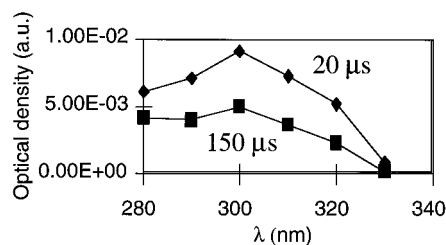


**Figure 3.** Transient absorption spectrum of aqueous benzene solution at 20  $\mu\text{s}$  and 150  $\mu\text{s}$  after the electron pulse ( $\text{N}_2\text{O}$ -saturated, 180  $\mu\text{M}$  benzene, 140  $^\circ\text{C}$ , 4150 psia, pH 5.10).

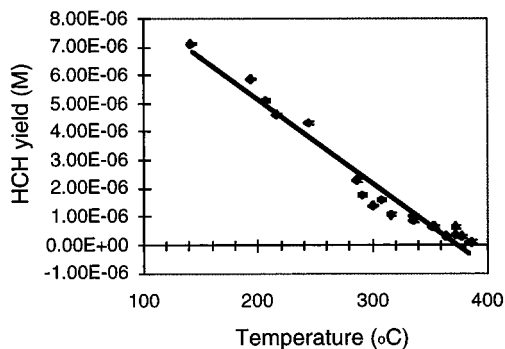


**Figure 4.** Effect of temperature on the initial yield of the HCH radical ( $\text{N}_2\text{O}$ -saturated, 180  $\mu\text{M}$  benzene, 140–385  $^\circ\text{C}$ , 4150 psia, pH 5.1).

of mechanisms:<sup>23,24</sup>



Production of hydrogen atoms was minimized by maintaining the pH above 3, and hydrated electrons were converted to hydroxyl radicals by saturating the aqueous solution with  $\text{N}_2\text{O}$ .<sup>25</sup>

**Benzene.** The reaction between benzene and  $\text{HO}^\bullet$  in water produces the hydroxycyclohexadienyl radical (HCH), a species with an absorption maximum at 312 nm ( $\epsilon_{312}$  1850  $\text{M}^{-1} \text{cm}^{-1}$ ).<sup>7</sup> Transient absorption spectra resulting from the pulse radiolysis of aqueous benzene in our cell (Figure 3) correspond to those previously reported for HCH.<sup>7</sup> The yield of HCH, measured immediately after the pulse between 140 and 385  $^\circ\text{C}$  (Figure 4), decreases linearly with temperature, with a slope of  $-2.97 \times 10^{-8} \text{ M}/^\circ\text{C}$  and a correlation coefficient of 0.96. No other transient was detected between 290 and 450 nm, which is consistent with previous reports that HCH alone is formed from this reaction between 20  $^\circ$  and 200  $^\circ\text{C}$ .<sup>26</sup> The observed decrease in yield may indicate that  $\text{HO}^\bullet$  reacted with benzene through a different mechanism at high temperature, perhaps producing a product that was unobservable under our experimental conditions. In addition, at high temperatures, HCH may have decayed so rapidly that only a portion of it survived beyond the initial pulse, causing an apparent decrease in yield.

An unusually large temperature dependence for the rate constant for the decay of HCH is observed, supporting this hypothesis. An Arrhenius plot over the temperature range from 140  $^\circ$  to 385  $^\circ\text{C}$  yielded a straight line (Figure 5), with  $E_a$  of 48.0 kJ/mol and a preexponential  $A$  value of  $7.42 \times 10^{14} \text{ M}^{-1} \text{ s}^{-1}$ .

The rate constant for the bimolecular decay of HCH does not track the rate of increase predicted for a diffusion-controlled reaction:

$$k = 8RT/3000\eta \quad (2)$$

where the units of  $k$  are  $\text{M}^{-1} \text{ s}^{-1}$ ,  $R$  is  $8.31 \times 10^7 \text{ erg (mol$

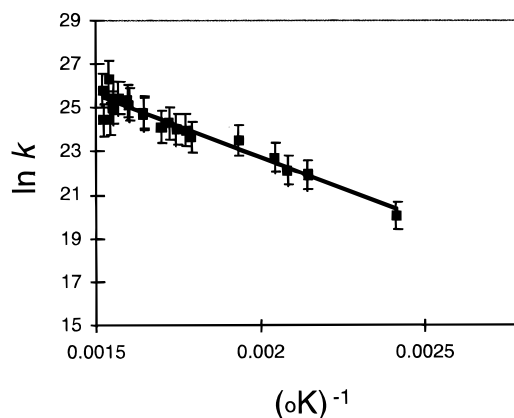


**Figure 5.** Arrhenius plot for the rate constant of the bimolecular decay of the HCH radical ( $\text{N}_2\text{O}$ -saturated, 180  $\mu\text{M}$  benzene, 140–385  $^\circ\text{C}$ , 4150 psia, pH 5.10).

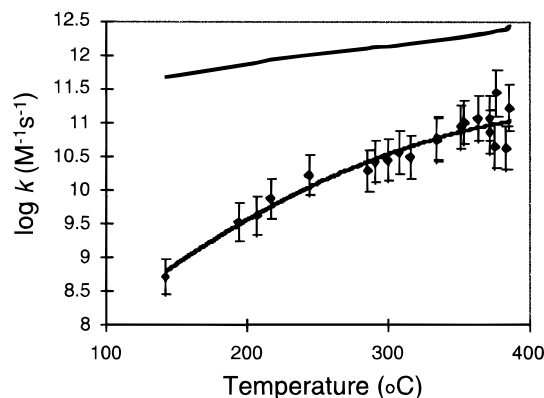


**Figure 6.** Comparison of the effect of temperature on the recombination rate constant of the HCH radical (bottom data set) with the theoretical effect of temperature on a diffusion-controlled reaction (solid line) ( $\text{N}_2\text{O}$ -saturated, 180  $\mu\text{M}$  benzene, 140–385  $^\circ\text{C}$ , 4150 psia, pH 5.1).

$\text{K}^{-1}$ , and  $\eta$  (viscosity) is in poise.<sup>27,28</sup> Rather, the value of the rate constants plateaued at high temperatures (Figure 6). Computer simulation of ion solvation at high temperatures suggests that the immediate solvent environment around the ion is similar to that found at room temperature, suggesting that the temperature dependence for the rate of diffusion in the microenvironment around the solute may be less than that predicted for the bulk phase.<sup>29</sup> Although diffusion kinetic theory predicts a similar plateauing of rate constants at high temperature for diffusion-controlled reactions, the high activation energy and linear Arrhenius relationship for this reaction are more consistent with reactivity control,<sup>30</sup> indicating that solvent clustering is the probable cause.

**Pentabromophenolate Anion.** The reaction of pentabromophenolate anion with  $\text{HO}^\bullet$  produces both the corresponding  $\text{HO}^\bullet$  adducts and the phenoxyl radical (Scheme 1).<sup>5</sup> From the known absorption maxima and extinction coefficients for each species,<sup>32</sup> the yields of each product were determined as a function of temperature. As with benzene, the yield of  $\text{HO}^\bullet$  adducts was temperature-dependent, decreasing linearly with temperature (correlation of 0.95 and a slope of  $-1.03 \times 10^{-9} \text{ M}/^\circ\text{C}$ ) (Figure 7). The yield of the pentabromophenoxyl radical appeared insensitive to temperature until the critical point was exceeded. However, the rapid change in solvent density at this point lowered the concentration of the pentabromophenolate anion below that necessary to ensure pseudo-first-order condi-

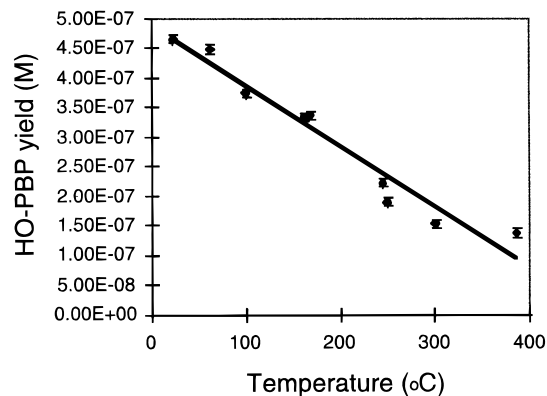


**Figure 7.** Effect of temperature on the yield of the HO<sup>•</sup> pentabromophenolate adduct (HO-PBP) (pentabromophenolate 100  $\mu$ M, dibasic phosphate buffer 500  $\mu$ M, solution pH 8.5, 4250 psia, degassed with N<sub>2</sub>O, 32–380 °C).

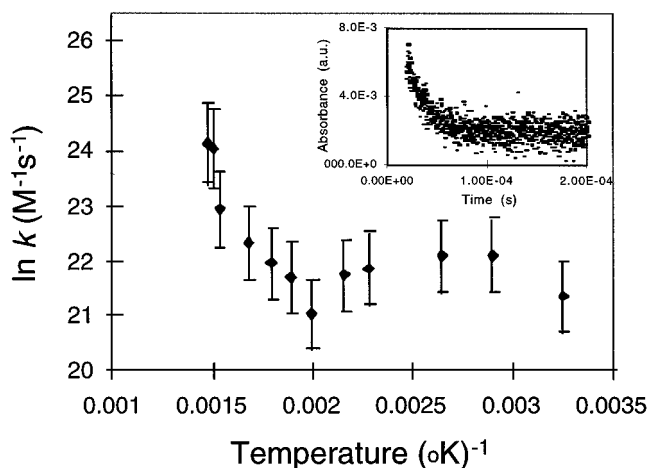


**Figure 8.** Arrhenius plot for the rate constant for the decay of the pentabromophenoxyl radical (pentabromophenolate 100  $\mu$ M, dibasic phosphate buffer 500  $\mu$ M, solution pH 8.5, 4250 psia, degassed with N<sub>2</sub>O, 32–405 °C). Inset: transient absorbance of the pentabromophenoxyl radical at 430 nm and 380 °C.

tions. The high ground-state absorbance of the halogenated anion precluded attempts to use higher initial substrate concentrations.

Since the reaction between pentabromophenolate and HO<sup>•</sup> produces roughly 25% HO adduct and 75% pentabromophenoxyl radical, the observed decay kinetics of the HO<sup>•</sup> adduct included contributions from its self-reaction and its reaction with the phenoxyl radical. However, the pentabromophenoxyl radical was present in excess at room temperature (relative to the HO<sup>•</sup> adduct), and that excess only grew at higher temperature. Therefore, the bimolecular rate constant for the decay of the pentabromophenoxyl radical was assigned to self-reaction. Accordingly, the rate constant for the decay of the pentabromophenoxyl radical was determined over the temperature range from 32 ° to 405 °C. The actual yield of pentabromophenoxyl radical remained constant over this range.

The temperature dependence of the rate constant for pentabromophenoxyl decay was non-Arrhenius over this temperature range (Figure 8). It remained essentially unchanged until 250 °C, where a sharp change in slope indicated a change in mechanism, although the decay was still best fit as a second-order process. Interestingly, a far more useful predictor for the rate constant was the bulk density of the aqueous solution.<sup>28</sup> A plot of the bulk density against the rate constant for the decay (Figure 9) had a correlation coefficient of 0.77.

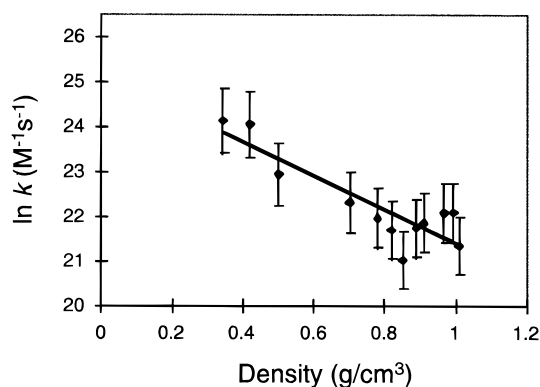


**Figure 9.** Density as a predictor of the pentabromophenoxyl radical decay rate (pentabromophenolate 100  $\mu$ M, dibasic phosphate buffer 500  $\mu$ M, solution pH 8.5, 4250 psia, degassed with N<sub>2</sub>O, 32–405 °C).

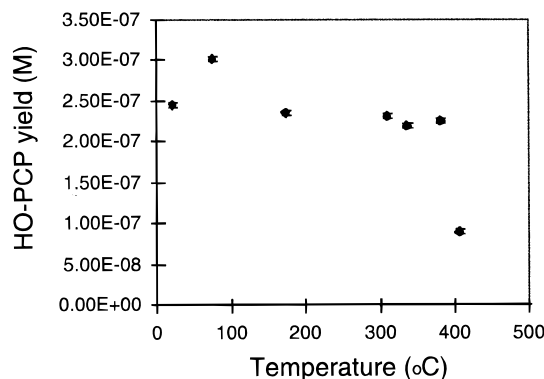


**Figure 10.** Effect of temperature on the yield of the HO<sup>•</sup> adduct of pentachlorophenolate (pentachlorophenolate 360  $\mu$ M, dibasic phosphate buffer 500  $\mu$ M, pH 9.5, 4300 psia, 35–380 °C, degassed with N<sub>2</sub>O).

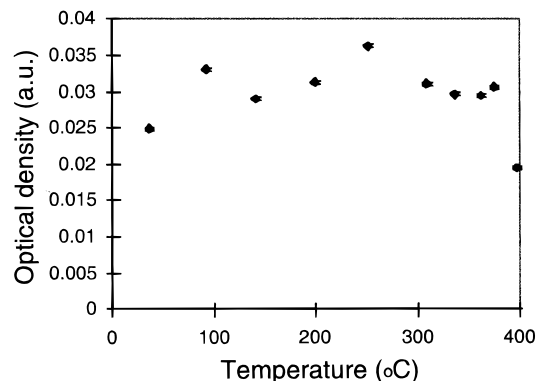


**Figure 11.** Effect of temperature on the transient absorbance at 450 nm generated during the reaction of HO<sup>•</sup> with pentachlorophenolate (pentachlorophenolate 360  $\mu$ M, dibasic phosphate buffer 500  $\mu$ M, pH 9.5, 4300 psia, 35–380 °C, degassed with N<sub>2</sub>O).

**Pentachlorophenolate.** The reaction between HO<sup>•</sup> and the pentachlorophenolate anion gives a product distribution of 23% HO<sup>•</sup> adduct and 77% phenoxyl radical.<sup>5</sup> The known extinction coefficients and yields were used to determine the effect of temperature on the yield of the *m*- and *o*-HO<sup>•</sup> adducts<sup>5</sup> (Figure 10). The yield of the perchlorinated HCH radical was essentially independent of temperature below 400 °C. The absorption spectra of the *p*-HO<sup>•</sup> adduct and the pentachlorophenoxyl radical overlap strongly, and quantitative deconvolution of the data on the yield of these species proved difficult. However, the transient absorption at 450 nm, where both the *p*-HO<sup>•</sup> adduct and the pentachlorophenoxyl radical absorb strongly,<sup>5</sup> remained essentially unchanged over the temperature range from 35 ° to

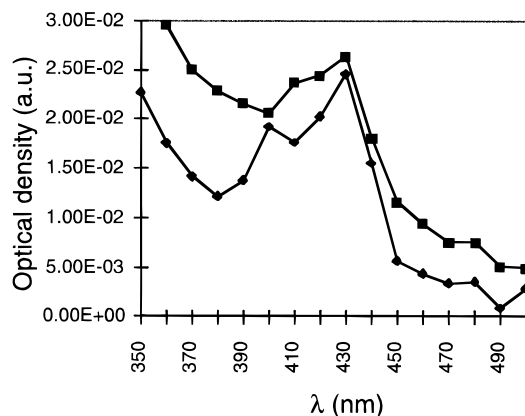


**Figure 12.** Transient absorption spectrum from the reaction of pentafluorophenolate with HO• at 22 °C (lower spectrum) and 290 °C (upper spectrum) (pentafluorophenolate 450  $\mu$ M, dibasic phosphate buffer 500  $\mu$ M, pH 8.56, degassed with N<sub>2</sub>O, 4300 psia).

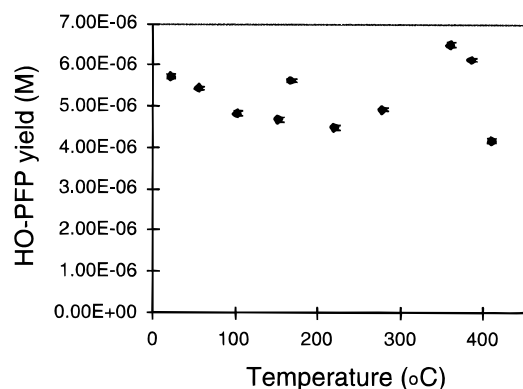


**Figure 13.** Effect of temperature on the yield of the HO• adduct to pentafluorophenolate (pentafluorophenolate 450  $\mu$ M, dibasic phosphate buffer 500  $\mu$ M, pH 8.6, degassed with N<sub>2</sub>O, 21–385 °C, 4300 psia).

380 °C (Figure 11), consistent with the findings for the pentabromophenoxy radical.

**Pentafluorophenolate.** The reaction between pentafluorophenolate anion and HO• has been reported to produce the HO• adduct<sup>5</sup> or the pentafluorophenoxy radical,<sup>33</sup> but not both. In this work, the transient absorption spectrum from the radiolysis of aqueous pentafluorophenolate anion at room temperature (Figure 12) matched that reported for the HO• adduct, with an absorption maxima at 430 nm, although the shoulder at 400 nm was more pronounced than previously reported,<sup>5</sup> indicating that there may be a mixture of products present. The yield of HO• pentafluorophenolate adduct was constant over the range from 20 ° to 410 °C (Figure 13). However, the transient absorbance in the 360–400 nm portion of the spectrum *increased* with temperature (Figure 12). This indicated the appearance of new products during the pulse, perhaps a mixture of different isomers of the HO• adduct or the pentafluorophenoxy radical.

It was not possible to measure the effect of temperature on the rate constant for the decay of the HO–pentafluorophenolate adduct. Although it was possible to observe the decay at low temperatures, at higher temperatures ( $T < 200$  °C) the transient signal appeared to be persistent (Figure 14). A possible explanation for this was that at high temperatures a stable product with a similar absorption spectrum to the HO• adduct may have been formed within the pulse, rather than any radical species.

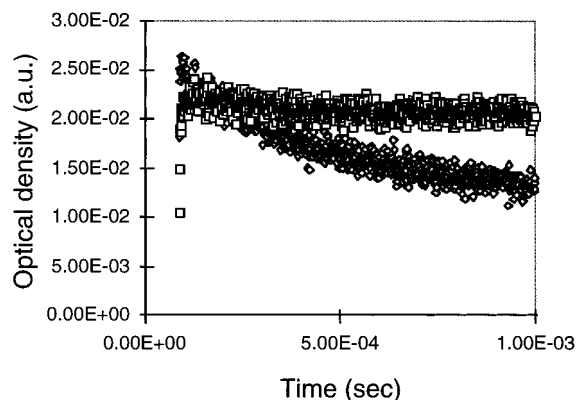


**Figure 14.** Effect of temperature on the decay rate of the HO• to pentafluorophenolate monitored at 430 nm: ( $\diamond$ ) 21 °C, lower trace; ( $\square$ ) 290 °C, upper trace (pentafluorophenolate 450  $\mu$ M, dibasic phosphate buffer 500  $\mu$ M, pH 8.1, degassed with N<sub>2</sub>O, 4300 psia).

## Conclusions

The yields of the HO• adducts to benzene, pentabromophenolate, and pentachlorophenolate decreased with increasing temperature, whereas the yields of the corresponding phenoxy radical seemed constant. This observation indicates that the mechanism by which the HO• adducts decay at high temperature did not involve the loss of hydroxide ion to generate the corresponding phenoxy radical.<sup>5,33</sup> Instead, a coupling mechanism may have been more important.<sup>2</sup> Although the local structure of the solvent around the solute may have influenced the decay kinetics of HCH and the pentabromophenoxy radical, it did not have any apparent effect on the product distribution. Rather, in all cases where it was possible to differentiate between products, temperature seemed to be the most successful predictor of product distribution.

**Acknowledgment.** This work was supported by the University Research Initiative of the U.S. Army Research Office and by the Texas Advanced Research Program. We would like to express our gratitude to Dr. Don O'Connor and Mr. Bill Naumann of the Center for Fast Kinetics Research for their considerable and patient assistance.

## References and Notes

- (1) Li, L.; Chen, P.; Gloyna, E. F. *AIChE J.* **1991**, *37*, 1687.
- (2) von Sonntag, C.; Schuchman, H. P. *Angew. Chem., Int. Ed. Engl.* **1991**, *30*, 1229.
- (3) Gopalan, S.; Savage, P. E. *J. Phys. Chem.* **1994**, *98*, 12646.
- (4) Crain, N.; Tebbal, S.; Li, L.; Gloyna, E. F. *Ind. Eng. Chem. Res.* **1993**, *32*, 2259.
- (5) Terzian, R.; Serpone, N.; Draper, R. B.; Fox, M. A.; Pelizzetti, E. *Langmuir* **1991**, *7*, 3081.
- (6) Terzian, R.; Serpone, N.; Fox, M. A. *J. Photochem. Photobiol. A: Chem.* **1995**, *90*, 125.
- (7) Gordon, S.; Schmidt, K. H.; Hart, E. J. *J. Phys. Chem.* **1977**, *81*, 104.
- (8) Mohan, H.; Mittal, J. P. *J. Phys. Chem.* **1995**, *99*, 6519.
- (9) Ye, M.; Schuler, R. *J. Phys. Chem.* **1989**, *93*, 1898.
- (10) Alfassi, Z. B.; Shoute, L. C. T. *Int. J. Chem. Kinet.* **1993**, *25*, 79.
- (11) Buxton, G. R.; Langan, J. R.; Lindsay-Smith, J. R. *J. Phys. Chem.* **1986**, *90*, 6309.
- (12) Olivella, S.; Sole, A.; Garcia-Raso, A. *J. Phys. Chem.* **1995**, *99*, 10549.
- (13) Shaw, R. W.; Brill, T. B.; Clifford, A. A.; Franck, E. U. *Chem. Eng. News* **1991**, *69*, 26.
- (14) Sealock, L. J.; Elliott, D. C.; Baker, E. G.; Butner, R. S. *Ind. Eng. Chem. Res.* **1993**, *32*, 1535.
- (15) Connolly, J. F. *J. Chem. Eng. Data* **1966**, *11*, 13.
- (16) Hrnjez, B. J.; Mehta, A. J.; Fox, M. A.; Johnston, K. P. *J. Am. Chem. Soc.* **1989**, *111*, 2662.
- (17) Fernandez, D. P.; Mulev, Y.; Goodwin, A. R. H.; Levelt-Sengers, J. M. H. *J. Phys. Chem. Ref. Data* **1995**, *24*, 33.

- (18) Michael, B. D.; Hart, E. J. *J. Phys. Chem.* **1970**, *74*, 2878.
- (19) Zhang, J.; Connery, K. A.; Strebing, R. B.; Brennecke, J. F.; Chateaufneuf, J. E. *Rev. Sci. Instrum.* **1995**, *66*, 3555.
- (20) Siskin, M.; Katritzky, A. R. *Science* **1991**, *254*, 231.
- (21) Jin, L.; Ding, Z.; Abraham, M. A. *Chem. Eng. Sci.* **1992**, *47*, 2659.
- (22) Xiang, T.; Johnston, K. P. *J. Phys. Chem.* **1994**, *98*, 7915.
- (23) Fahrataziz, M. A. Rodgers, Eds. *Radiation Chemistry, Principles and Applications*; VCH Publishers: New York, 1987.
- (24) Spinks, J. W. T.; Woods, R. J. *An Introduction to Radiation Chemistry*; Wiley-Interscience: New York, 1990.
- (25) Buxton, G. V.; Greenstock, C. L.; Helman, W. P.; Ross, A. B. *J. Phys. Chem. Ref. Data* **1988**, *17*, 513.
- (26) Ashton, L.; Buxton, G. V.; Stuart, C. R. *J. Chem. Soc., Faraday Trans.* **1995**, *91*, 1631.
- (27) Gordon, A. J.; Ford, R. A. *The Chemist's Companion*; Wiley-Interscience: New York, 1972; p 137.
- (28) Gallagher, J. S.; Haar, L. *NIST Standard Reference Database 10, Steam Table*, Department of Commerce, 1985.
- (29) Tanger, J. C.; Pitzer, K. S. *J. Phys. Chem.* **1989**, *93*, 4941.
- (30) Elliot, A. J.; McCracken, D. R.; Buxton, G. V.; Wood, N. D. *J. Chem. Soc., Faraday Trans.* **1990**, *86*, 1539.
- (31) Ekart, M. P.; Brennecke, J. F.; Eckert, C. A. In *Supercritical Fluid Technology, Reviews in Modern Theory and Applications*; Bruno, T. J., Ely, J. F., Eds.; CRC Press: Boca Raton, FL, 1991; p 164.
- (32) Reference 5 gives  $\lambda_{\max}$  for the HO<sup>•</sup> adduct at 400 nm as  $\epsilon_{400}$  11 000 M<sup>-1</sup> cm<sup>-1</sup> and  $\lambda_{\max}$  for the pentabromophenoxy radical at 470 nm as  $\epsilon_{470}$  3200 M<sup>-1</sup> cm<sup>-1</sup>.
- (33) Shoute, L. T.; Mittal, J. P. *J. Phys. Chem.* **1993**, *97*, 379.